Flow Field and Mass Flux Measurements Near the Exit Plane of Spray Jets

J. D. Gounder* and A. R. Masri
School of Aerospace, Mechanical and Mechatronic Engineering
The University of Sydney
NSW 2006 AUSTRALIA

Abstract

This paper provides velocity as well as mass flux measurements in a number of spray jets with varying droplet loading. A simple burner geometry consisting of a contraction and an annular pilot holder with an ultrasonic nebulizer mounted 215mm upstream of the jet exit plane was used. The spray particles are entrained in the carrier air at this upstream location with zero momentum such that the complexities of the atomization process are avoided and well defined boundary conditions can be obtained at the jet exit plane. A mineral turpentine spray jet was used as a base case to emulate non-evaporating conditions. Liquid mass flow rates of 0.0234, 0.045 and 0.075 kg/min were used as low, medium and high spray loading cases respectively. The carrier bulk velocity was fixed at 24 m/s. When conditioned with respect to droplet size, an anomaly was found in the measurements of turbulence at radial locations close to the jet wall: the rms fluctuations for larger droplets were higher than those for the smaller droplets. Probability density function plots of velocity near the wall reveal a bimodal distribution, which changes gradually to a monomodal one as the jet centerline is approached. This bimodality is believed to be caused by droplets impacting the inner surface of the nozzle and slowed in the boundary layer. This effect is magnified with droplet size leading to the artificially higher rms at the exit plane. The bimodal pdf is then reconstructed where possible into two single-mode pdfs corresponding, respectively, to the droplets affected by the wall and those unaffected. The new rms fluctuations of the velocities obtained from the single-mode pdf of large droplets is no longer higher than the rms of small droplets and hence more akin to what is expected of turbulence fluctuations.

Introduction

Spray flows remain poorly understood despite their prominence in a wide range of industrial application such as internal combustion engines, turbines and industrial burners. In order to enhance current understanding of the complex features of spray flows, extensive experimental measurements as well as numerical simulations need to be performed. Direct research in practical spray flows is generally hindered by complex boundary conditions as well as the difficulty of performing measurements. The study of complex phenomena such as evaporation of droplets, turbulent dispersion and turbulence modulation of the gas phase flow due to the presence of droplets is best performed in laboratory-type model burners with simple well defined boundary conditions.

The spray burner at Sydney University has been designed with the objective of establishing it as a modal burner with simple boundary conditions that can provide extensive data for the purpose of testing and validating numerical models. Using an early version of the burner Chen and Starner [1-3] studied the effect of turbulence on evaporation in sparsely loaded spray jets of acetone, where a glass nebulizer was used to create fine spray with Sauter mean diameter ranging from 14 to 35 microns. In later work by Starner et al [4, 5] a modified version of the spray burner was used, for studying non reacting and reacting spray jet of acetone, where the spray droplets were generated using an ultrasonic nebulizer with Sauter mean diameter around 40 microns, which is more akin to sprays in industrial applications. Nijdam *et al* [6] investigated the effect of droplet evaporation and coalescence. Sommerfeld and Qiu [7] have studied evaporation of sprays in heated jets and there are others [8-11] who have carried out work on turbulent dispersion and turbulence modulation of gas flow by droplets.

In this paper velocity and turbulence fields as well as droplet fluxes are measured at the exit plane of spray jets using Phase Doppler Particle Anemometry and Laser Doppler Velocimetry technique. An anomaly with respect to the rms velocity fluctuations for large droplets near the jet wall is discovered and resolved.

Experimental Setup

The spray burner consists of a smooth contraction and an annular pilot flame holder with an ultrasonic nebulizer mounted 20 diameters upstream of the exit plane, where the nozzle diameter is 10.5 mm and the 25 mm outer tube

*Corresponding author, james.gounder@aeromech.usyd.edu.au

forms the annular pilot flame holder. Figure 1 shows a detailed schematic of the burner and co-flow assembly. The burner assembly is mounted in a vertical wind tunnel. The tunnel exit has a cross section of 29 cm by 29 cm and supplies filtered co-flowing air stream at 4.5 m/s with low turbulence intensity. A 104 mm diameter co-flow surrounds the burner. A series of perforated steel plates, honey comb and screens have been used to produce uniform velocity of 4.5 m/s with low turbulence at the exit plane of the co-flow. Ultrasonically generated droplets of acetone with zero momentum are entrained into the carrier stream. The flow rates of carrier air and acetone are regulated using rotameters.

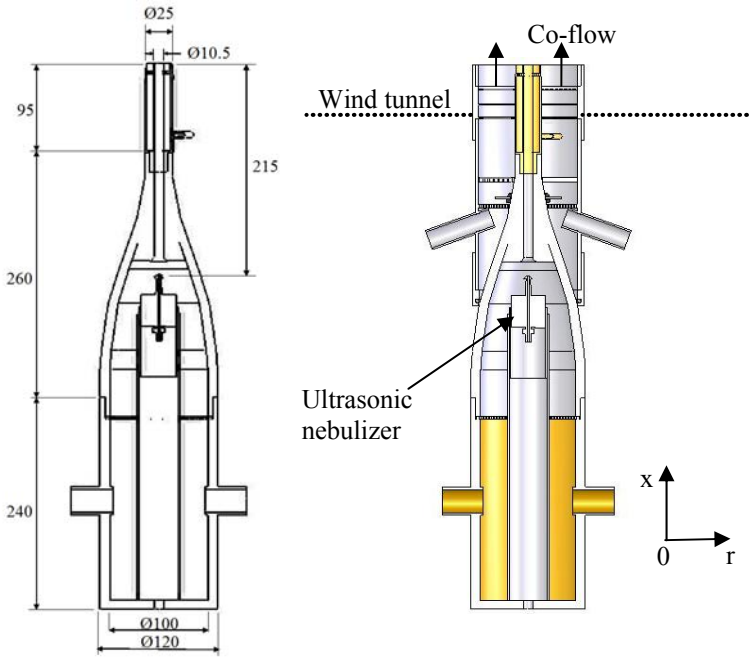

Figure 1. Configuration of the Spray Burner

Three acetone spray jets with increasing droplet loadings were investigated. The bulk jet velocity of the carrier air was kept constant at 24m/s. These jets have been labeled SP1, SP3 and SP4, where case SP1 is the highest loading and case SP4 the lowest. The liquid acetone injection rates are 94.9, 57.0 and 29.6 ml/min for jets SP1, SP3 and SP4, respectively. Mineral turpentine ('Turps') was used as a base case due to its high boiling point to emulate a non evaporating jet. The liquid volume flow rate of mineral turpentine was 26.9 ml/min. A K-type thermocouple with a bead diameter of 1 mm was used for measuring gas phase temperature at the nozzle exit plane.

The phase-Doppler anemometer (TSI Model FSA 3500/4000) is arranged in the 45^{o} forward scattering mode with 300 mm receiver focal length and 3.2 mm fringe spacing. An Argon-ion laser feeds the fiber optics assembly. The photomultiplier voltage is set at 395 V. Two components of the velocity, axial U and radial V of droplets, droplet diameter, droplet number density and droplet volume flux are measured in radial traverses of the jet, at normalized axial locations x/D = 0.3, 5, 10, 15, 20, 25 and 30 downstream of the nozzle exit plane. To maximize the quality of the flux measurements, only the axial velocity is measured together with the size data, this yielded the highest size validation percentage. Two channel velocity and size measurements were collected separately to obtain radial velocity and shear stress data. Software coincidence has been applied on velocity measurements together with the intensity validation scheme applied to drop size measurements. The built in probe volume correction (PVC) has been implemented to correct for lower visibility of small droplets at the edge of the measurement volume. All parameter settings of the receiver optic assembly were maintained constant throughout the length of the jet in order to minimize any bias towards size distribution relative to upstream results. These settings are thus determined by the saturation constraints at the jet exit.

Results and Discussion

The low boiling point of acetone (56^{o} C at atmospheric pressure) makes it a good candidate for studying evaporation of sprays. In order to gain confidence in the flux measurements in evaporating spray jets using PDPA, valida-

tion is performed against a non-evaporating jet case where mineral turpentine is used and the droplet flow rate is obtained by integrating measured droplet fluxes across the jet at the exit plane. Given that mineral turpentine has a high boiling point, such measurements should yield a mass flux almost equal to the injected flow rate. The droplet flow rate for the mineral turpentine case at the exit plane was 24.6 ml/min. For the acetone spray cases SP1, SP3 and SP4 the measured droplet flow rate at the exit plane are 27.1, 20.4 and 12.9 ml/min, respectively. Any reduction in the droplet flow rate of the acetone jets is due to evaporation. This is further confirmed by the low temperatures of the gas phase measured at the exit plane, which are -1.76, -6.18 and -5.80 ^{o}C respectively for cases SP1, SP3 and SP4. The droplet flow rates obtained by integration of measured fluxes across the jet at each axial location for the mineral turpentine case as well as acetone case SP4 are shown in Figure 2. As expected, the total mass flux for mineral turpentine for all droplet sizes is well conserved whereas acetone case SP4 shows the decay in droplet flow due to evaporation. The results when conditioned on droplet size show the mass transfer between different droplet sizes. Measurements in the mineral turpentine case recover over 90% of the injected liquid flow at all axial locations. This verifies that the PDPA/LDV setup is optimized for measuring accurate droplet flux as well as velocities in an evaporating jet.

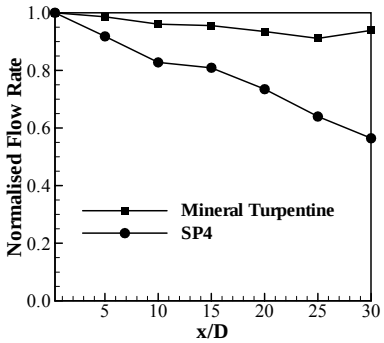

Figure 2. Total droplet flow rates, normalized by values at the jet exit plane for non-evaporating spray jet of mineral turpentine and evaporating acetone spray jet SP 4.

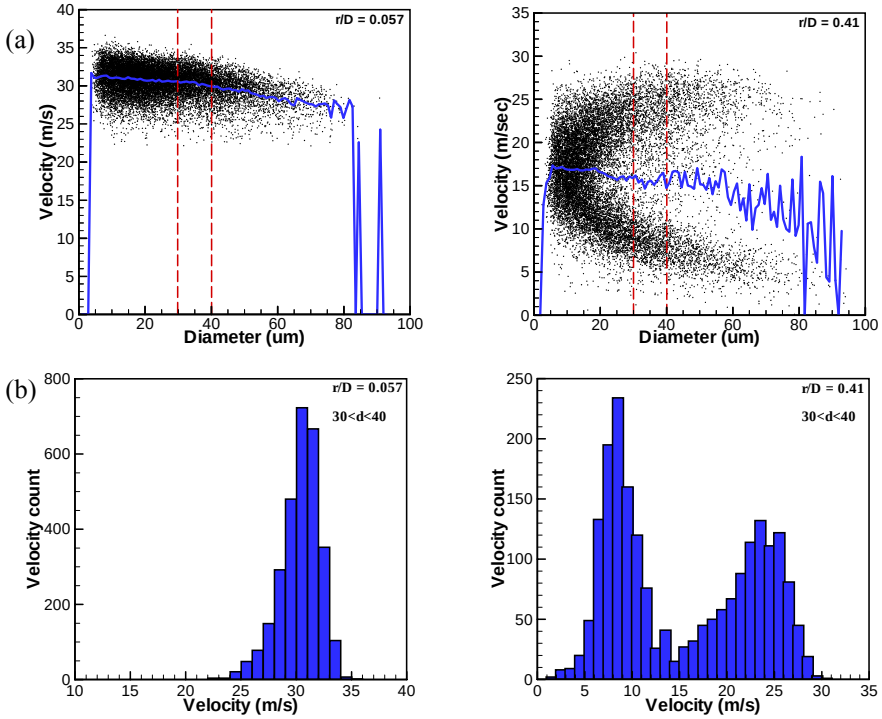

Figure 3. (a) Scatter plot of instantaneous velocity verses diameter at radial positions, r/D = 0.057 and 0.41. **(b)** Velocity probability density function (pdf) for droplet in the diameter range 30<D<40 μm.

Small droplets have lower inertia compared with larger ones, and thus follow the turbulent fluctuations of the gas flow more closely. Droplets smaller than 10 μm were shown [2] to have velocities close to that of the gas phase. As the droplet diameter increases, the inertia of the droplets increase as well and hence their tendency to maintain their speed; such large droplets are less likely to respond to flow turbulence fluctuations. In the present work as well as in earlier work done by Starner *et al* [4] in turbulent spray flames of acetone, rms fluctuations for the axial velocity measured for large droplets near the wall at the jet exit plane where higher than those measured for droplets smaller than 10 μm. This is anomalous and contrary to expectation.

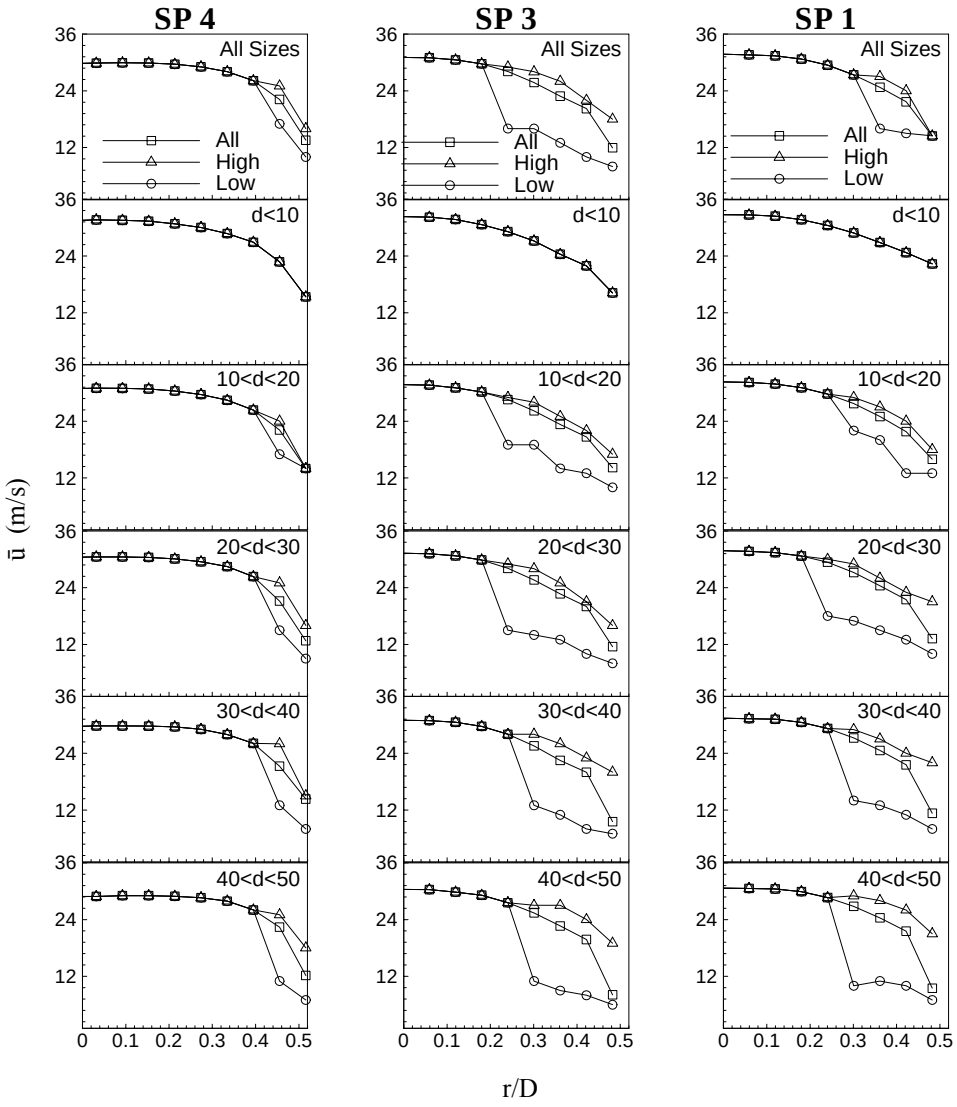

Figure 4. Radial profile of mean axial velocity (ū) conditioned on droplet diameter. The edge of the jet shows mean velocity from the bimodal velocity pdf represented by 'All' and the 'High' and 'Low' mean velocity obtained from the peaks of the bimodal pdf.

In exploring this issue further, the scatter plots for the instantaneous realizations of velocity versus droplet diameter measured at two radial locations are shown in Fig. 3. Close to the center of the jet at r/D = 0.057 the velocity scatter for all size particles is close to the mean velocity expected of a fully developed turbulent flow. The mean velocity of the individual diameter bins reduces as the particle diameter increases. This is expected as small particles have larger drag coefficients and thus small relaxation times leading to greater droplet accelerations and thus exit the nozzle with zero slip velocity. On the other hand larger droplets with greater inertia have longer relaxation time thus

exiting the nozzle with negative slip velocities. As the nozzle wall is approached, the scatter plots for velocity show a bimodal distribution with the bimodality becoming more distinct for larger droplets. Figure 3(b) shows the velocity pdf for droplets in the size range 30 to 40 μm. Close to the jet centerline, the pdf is mono-modal and gradually shifts to a bimodal distribution as the jet wall is approached. Droplets with higher velocities (top branch of the velocity distribution) are those that remain unaffected by the presence of the solid wall while slower droplets appear to have been slowed down by the boundary layer forming on the inner surface. It is this bimodality that leads to the artificially high rms velocity fluctuations measured for larger droplets near the jet wall.

The true rms fluctuations of the large droplets near the jet wall may be obtained by separating the bimodal branches of the pdf and obtaining the rms of each branch separately. This is achieved as follows: for the high velocity branch, the distribution on the right hand side of the peak is taken as a true representation of the full distribution by assuming symmetry and hence forms the basis for calculating the mean and rms fluctuations. For the low velocity branch, the same approach is used except that the distribution on the left hand side of the peak is now used. Radial locations where the peaks of the pdf could not be delineated have been left alone. Using this approach, the mean and rms fluctuations may be calculated using the low velocity branch or the high velocity branch or both together.

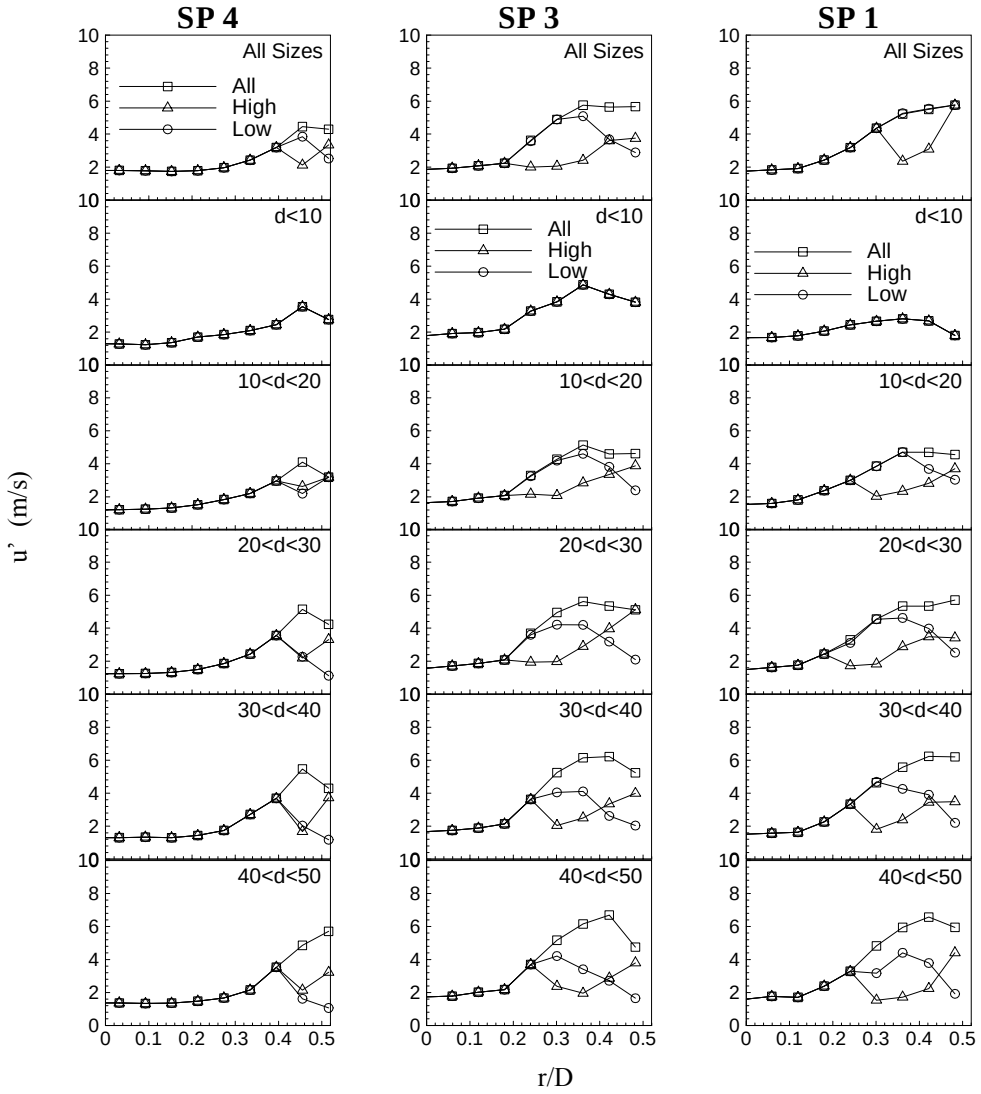

Figure 5. Radial profile of axial rms velocity (u') conditioned on droplet diameter. Also present are the local rms calculated from reconstructed velocity pdfs.

Figures 4 and 5 show, respectively radial profiles of the mean and rms fluctuations of the axial velocity conditioned on droplet diameter for cases SP1, SP3 and SP4. Results are shown for six sizes of droplets and for each bin size, three sets of mean velocities are shown at the edge of the jet: 'All' in the figure stands for mean velocity of all particles ie the mean of the bimodal pdf while "High" and "Low" refer respectively to the high velocity and low velocity branches of the distribution. For the three spray jets investigated here the Stokes number for droplets smaller than 10 μm lies in the range 0.05 to 0.08. Since the Stokes number is less than unity, the mean velocity and rms velocity profile of droplets smaller than 10 μm can represent the gas phase. The slip velocity of droplets larger than 50 μm varies from 2 to 3 m/s with decreasing droplet loading. Plots in Fig.4 show clearly that as the droplet size increases, the effects of the wall become larger in slowing those droplets down.

As seen in the scatter plots in figure 3(a), small droplets less than 10 μm in diameter do not show bimodality in the velocity pdf for all cases investigated here. Larger droplets start to show this bimodality as the jet wall is approached and for those cases the pdf is reconstructed as discussed earlier. It is evident from the profiles shown in figure 5, for the rms velocity fluctuations corresponding to the high and low branches of the pdf that the turbulence for large droplets is lower than those measured for small droplets as consistent with expectations. For droplets in the diameter range 10 to 50 microns, the rms fluctuations calculated for the high and low velocity branches, are lower than the gas phase. As the droplet size increases the calculated true rms close to the jet wall decreases and is lower than the rms velocity of droplets smaller then 10 μm. The stokes number for the three cases range between 0.05 to 1.67 and droplets between 10 and 30 microns have Stokes number less than one suggesting that there would be some similarities in the behavior of these droplets and gas phase. It is evident from these results that the high rms fluctuations noted earlier from the full distribution is indeed an artifact of the experiment due to the wall effect

Conclusion

A non evaporating spray jet of mineral turpentine was used for validating the accuracy and reliability of PDPA equipment. Over 90 % of the injected Mineral turp was collected at the exit plane. The droplet flow rate obtained by integrating the flux at axial locations downstream of the exit plane is well conserved for the turp case. The PDPA set up was then used for evaporating acetone jets of increasing droplet loading and the measured droplet flow rates at the exit plane suggest significant evaporation taking place.

The velocity measurements show a bimodal velocity pdf close to the jet wall for the three spray jets being studied. This resulted in artificially higher rms fluctuations for large droplets. The bimodality in the velocity pdf is due to larger droplets being affected by the boundary layer forming on the wall. The rms velocity fluctuations for the lower and the higher branches behave as expected where large droplets $40<d<50$ μm have lower rms thn the gas phase turbulence. As the droplet diameter decreases the turbulence fluctuation increases.

Acknowledgement

This work is supported by a grant from Australian Research Council.

References

1. Chen, Y.C., Starner, S.H., and Masri, A.R., *14th Australasian Fluid Mechanics Confrence*, Adelaide, Australia, 2002 December, pp. 267-270.
2. Chen, Y.C., Starner, S.H., and Masri, A.R, *Twenty-Ninth International Symposium on Combustion*, Sapporo, Japan, 2002 July, pp. 625-631.
3. Chen, Y.C., Starner, S.H., and Masri, A.R, *International Journal of Multiphase Flow* 32(4): 389-412(2006).
4. Starner, S.H., Gounder, J. D., and Masri, A.R., *Combustion and Flame* 143(4): 420-432 (2005).
5. Starner, S.H. and Masri, A.R., *9th International Conference on Liquid Atomization and Spray Systems*, Sorrento, Italy, 2003 .
6. Nijdam, J., Starner, S.H. and Langrish, T., *Experiments in Fluids* 37(4):504-517(2004).
7. Sommerfeld, M., and Qiu, H.H., *International Journal of Heat and Fluid Flow* 19(1):10-22(1998).
8. Durst, F. and Ruck, B., *Experiments in Fluids* 5(5):305-314(1987).
9. Ferrand, V., Bazile, R., Boree, J., and Charnay, G., *International Journal of Multiphase Flow* 29(2):195-217(2003).
10. Fleckhaus, D., Hishida, K., and Maeda, M., *Experiments in Fluids* 5(5):323-333(1987).
11. Yuan, Z. and Michaelides, E.E., *International Journal of Multiphase Flow* 18(5):779-785(1992).